

Inspection of embedded internal features in additively manufactured metal parts using metrological x-ray computed tomography

Felix H. Kim¹, Herminso Villarraga-Gómez², and Shawn P. Moylan¹

¹Production Systems Group

¹National Institute of Standards and Technology

Gaithersburg, MD, USA

²X-Ray/CT Group

Nikon Metrology, Inc.

Brighton, MI, USA

INTRODUCTION

Advances in metal additive manufacturing (AM) have made it possible to build parts with complex geometry. Metal AM has a high potential to impact various industries including aerospace and automotive. Complex interior features can be designed to reduce weight and improve mechanical or thermal efficiency of the components. These features, however, are generally inaccessible from the outside to vision-based inspection techniques for quality control. Undesirable interior defects such as porosity and cracks can be formed due to sub-optimal processing parameters, poor feed stock material quality, or environmental effects [1-3]. The mission-critical structural components require thorough inspections for defects and dimensional accuracies.

X-ray Computed Tomography (XCT) – based inspection is becoming a viable option for several manufacturing industries. XCT shows a clear three-dimensional (3D) internal structure of the part in inspection. XCT has been popularly used to understand materials structure and behavior [e.g., 4, 5]. As the technique is applied to industrial inspection settings, guidelines must be established prior to widespread adoption of the technique.

To establish XCT as a reliable non-destructive evaluation tool for inspections of fracture-critical components, it is important to determine the base-line detectability of AM defect types and sizes using XCT. Probability of Detection (PoD) is a measure used to determine the capability of

a non-destructive evaluation (NDE) technique. There are yet undetermined aspects of PoD and minimum detectable flaw size for typical flaws found in AM-produced parts using XCT. Only a handful of papers related to this topic have been published to date [6]. One of the critical steps in evaluating non-destructive inspection techniques including XCT will be the ability to test parts with intentionally placed simulated flaws inside AM-produced parts. Reliable artifacts with internal features that are representative of the defects occurring in AM need to be developed. Building an internal structure, however, is difficult with any conventional technique. AM, on the other hand, provides an opportunity to embed complex internal structures.

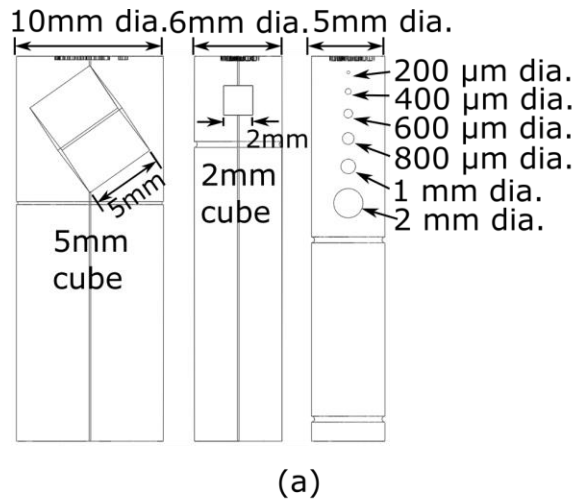
In this paper, an approach to build internal features using AM and to inspect the results using XCT are presented. Three test parts incorporating different internal features were built by a laser-based powder bed fusion (PBF) process. The qualities of these builds were determined from XCT scans. Metrological XCT scans measured the size of the internal features more accurately. The interior features were directly compared with the relevant computer-aided design (CAD) models. Based on the results, an improved artifact design is proposed.

LASER-BASED POWDER BED FUSION ADDITIVE MANUFACTURING OF SAMPLES WITH INTERNAL FEATURES

The parts were produced using laser-based PBF AM processes with a system (EOS M270) available at the National Institute of Standards

¹ Official contribution of the National Institute of Standards and Technology (NIST); not subject to copyright in the United States. The full descriptions of the procedures used in this paper require the identification of certain commercial products. The inclusion of such information should in no way be construed as indicating that such products are endorsed by NIST or are recommended by NIST or that they are necessarily the best materials, instruments, software or suppliers for the purposes described.

and Technology (NIST). Nickel-based super alloy (Inconel 625) powder (between 15 μm and 60 μm in particle size as measured by standard sieves) was used. The laser spot size is approximately 100 μm , and the default machine parameter settings were used for the material. Three samples were designed with interior features incorporating different sizes and orientations of cubes and spheres, as shown in FIGURE 1. Un-melted powders are expected to be trapped in the voids. The outer diameters of the samples are 10 mm, 6 mm, and 5 mm, respectively.



(b)

FIGURE 1. Designs of the samples with different internal features (a) and picture of the samples after the build (b).

X-RAY CT INSPECTION

Metrological XCT

Metrological XCT measurements were obtained for the three samples using an XCT system (Nikon XT H 225 ST). One of the main advantages of metrological XCT is the use of calibrated voxel size. Typical XCT techniques

estimate voxel size based on magnification factor alone. However, there is potential for dimensional errors with this approach due to axis position errors, geometric alignment error of CT system hardware, and X-ray focal spot drift error. Further, image quality can be affected by physical factors such as beam hardening and the scattering of X-rays, which need to be either prevented by hardware filtering or compensated with post-processing corrections after CT reconstruction.

For the current measurement, a calibration of the voxel size and a beam hardening correction were performed. The voxel size calibration is achieved in a similar fashion to the guidelines from [7] by running a CT scan of a calibration object (FIGURE 2) with the identical scan settings to those used in measuring the test pieces. The calibration object is a hollow aluminum cylinder, which was measured with a coordinate measurement machine (CMM) to obtain reference dimensions. The XCT scan parameters are shown in TABLE 1. Slight differences between the effective voxel size calculated based on uncalibrated geometric magnification and the calibrated voxel size are noticed.

For CT measurements, the samples were mounted at an angle of 20° from the vertical axis to avoid cone-beam artifacts.

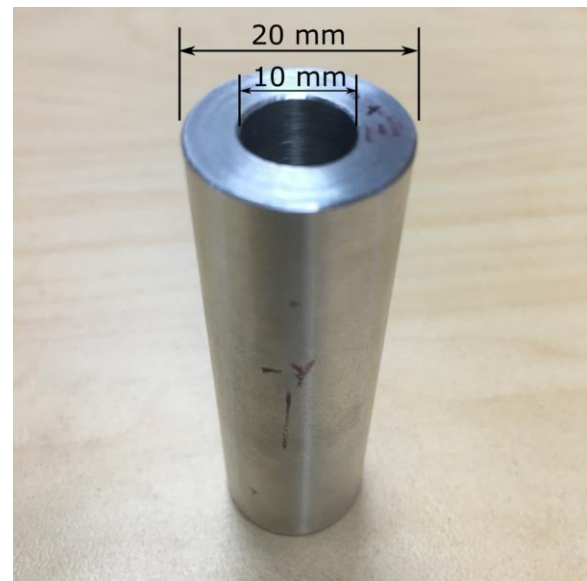


FIGURE 2. XCT calibration object

TABLE 1. XCT scan parameters

Sample	Large Cube	Small Cube	Sphere
Voltage (kV)	200	180	180
Current (μ A)	91	90	90
Power (W)	18.2	16.2	16.2
Filter Type and Thickness	Copper 3 mm	Copper 3 mm	Copper 3mm
Exposure Time (ms)	1000	1000	1000
Number of Projections	2880	2880	2880
Frame Per Projection	1	1	1
Detector Pixel Size (μ m)	200	200	200
Geometric Magnification	14.29	15.32	15.32
Magnification-based Voxel Size (μ m)	14.00	13.06	13.06
Calibrated Voxel Size (μ m)	14.05	13.08	13.08
Percent Difference (%)	0.36	0.15	0.15

Feasibility of Building Internal Features

Vertical interior slices at about the midsection of each sample are shown in FIGURE 3. High contrast of the solid parts was achieved, and the voids filled with powders can be easily distinguished from the solidified structure. The powder-trapping void looks darker due to porosity and the fairly coarse spatial resolution compared to the powder size.

In the sphere sample, the 200 μ m diameter spherical pore was not built. At the current XCT spatial resolution, no visible pore is found in the area. Both the spheres and the small cube experienced difficulties with producing accurate top surfaces. On the other hand, the large cube was built relatively well despite the larger overall dimensions. Small (100 μ m dia.) holes were designed and incorporated for the purpose of possibly getting the powders out, but they also did not appear to be built. Unintentional pores were not visible in the XCT images at the spatial resolution used, which confirms that the AM

processing parameters used were optimal to reduce porosity formation.

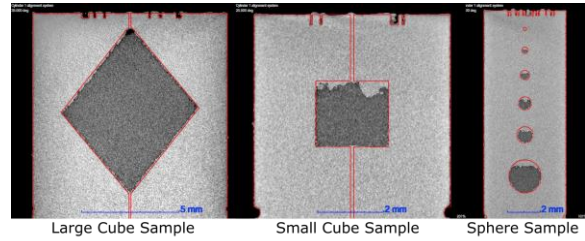


FIGURE 3. Results of metrological XCT scans and CAD overlaid.

Nominal to Actual Comparison

The metrological XCT images were directly compared to the CAD drawings as shown in FIGURE 4, 5, and 6. The XCT surface was registered to CAD via an iterative best-fit algorithm. The nominal geometry locations were subtracted from the actual position in the surfaces determined from XCT volumes. The deviations from the nominal geometry were as large as about $\pm 100 \mu$ m, and the locations with deviations larger than $\pm 50 \mu$ m are highlighted as red and magenta in the inner figures.

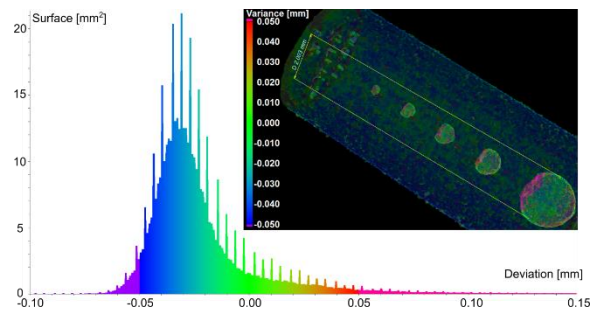


FIGURE 4. Part-to-CAD comparison showing the variance distribution for deviations of the CAD model for the sphere sample.

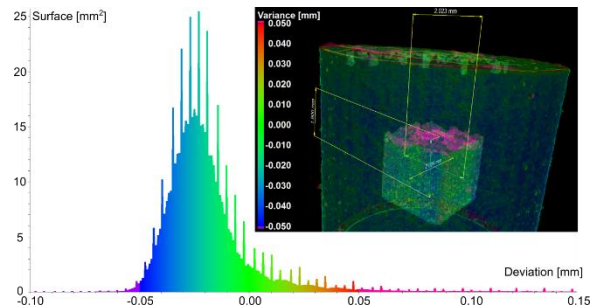


FIGURE 5. Part-to-CAD comparison showing the variance distribution for deviations of the CAD model for the small cube sample.

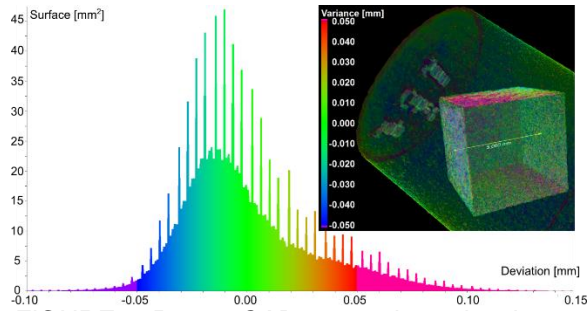


FIGURE 6. Part-to-CAD comparison showing the variance distribution for deviations of the CAD model for the large cube sample.

The nominal and actual volumes of the internal features are compared in TABLE 2. The difference between the nominal and actual volumes increased as the interior feature size decreased. The actual volumes were always smaller than the nominal volumes for the chosen designs due to inaccurate production of the top surfaces.

TABLE 2. Nominal and actual volumes of voids

	Nominal (mm ³)	Actual (mm ³)	Difference (%)
Large Cube	125	122.064	2.349
Small Cube	8	7.282	8.975
Sphere (2 mm dia.)	4.189	3.628	13.388
Sphere (1 mm dia.)	0.524	0.417	20.359
Sphere (0.8 mm dia.)	0.268	0.199	25.769
Sphere (0.6 mm dia.)	0.113	0.078	31.033
Sphere (0.4 mm dia.)	0.034	0.017	49.269

Improved Design

Based on the XCT images of the initial prototypes, an improved design is proposed to be built as an artifact for determining PoD, and an example design is shown in FIGURE 7. The design involves cubes of different sizes that are

in rotated orientations. The cubes in this orientation are expected to be built closer to the nominal designs. Subsequent XCT measurements are planned for the new design.

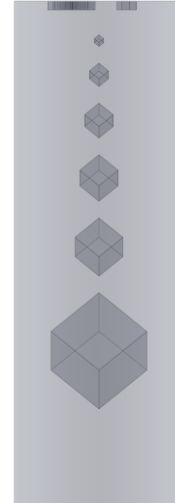


FIGURE 7. An improved design of test artifact

CONCLUSIONS

Samples incorporating internal features were built, and metrological XCT scans were obtained for the samples. The XCT scans were aligned with nominal CAD drawings for a direct comparison. Deviations up to ± 0.1 mm were detected between the nominal and measured dimensions of the AM-produced parts using XCT. Typical uncertainties of the CT measurements are in the order of 10 μm , which is a factor of five smaller than the measured deviation. Therefore, the ± 50 μm -tolerances are predominantly related to the AM process rather than the measurement uncertainty.

XCT has the ability to generate geometric data for characterization of material structures (internal and external features) and detect manufacturing defects and dimensional deviations from CAD design. To study complex structures produced by the additive manufacturing process, XCT is becoming a viable option to extract component dimensions of inner or hidden structures in a non-destructive manner. The XCT measurements also provided insights on building and embedding internal features using metal PBF processes. The metrological XCT of the controlled specimens provides good base-line data for measuring internal features. The obtained results can ultimately be used to quantitatively determine detectability of internal features using XCT.

Future plans include obtaining additional XCT images from different XCT systems for a comparison. Once all XCT scans are completed, a destructive measurement will be performed.

ACKNOWLEDGEMENTS

The authors would like to thank Mr. Mike McGlaulin of NIST for providing advice on developing a sample design, and Dr. Jarred Heigel of NIST for producing the parts with additive manufacturing.

REFERENCES

- [1] Ng GKL, Jarfors AEW, Bi G, Zheng HY. Porosity formation and gas bubble retention in laser metal deposition. *Appl Phys A*. 2009;97:641-9.
- [2] Thijs L, Verhaeghe F, Craeghs T, Humbeeck JV, Kruth J-P. A study of the microstructural evolution during selective laser melting of Ti-6Al-4V. *Acta Mater*. 2010;58:3303-12.
- [3] Yadroitsev I, Thivillon L, Bertrand P, Smurov I. Strategy of manufacturing components with designed internal structure by selective laser melting of metallic powder. *Appl Surf Sci*. 2007;254:980-3.
- [4] Maire E, Withers PJ. Quantitative X-ray tomography. *Int Mater Rev*. 2014;59:1-43.
- [5] Withers PJ, Preuss M. Fatigue and Damage in Structural Materials Studied by X-Ray Tomography. *Annual Review of Materials Research*. 2012;42:81-103.
- [6] Amrhein S, Rauer M, Kaloudis M. Characterization of Computer Tomography Scanners Using the Probability of Detection Method. *JNE*. 2014;33:643-50.
- [7] Lifton JJ, Malcolm AA, McBride JW, Cross KJ. The Application of Voxel Size Correction in X-ray Computed Tomography for Dimensional Metrology. 2nd Singapore International Non-destructive Testing Conference & Exhibition. Marina Bay Sands, Singapore 2013.